THE JOURNAL OF PHYSICAL CHEMISTRY B

Article

pubs.acs.org/JPCB

Dewar Lesion Formation in Single- and Double-Stranded DNA is Quenched by Neighboring Bases

Dominik B. Bucher,[†,‡] Bert M. Pilles,[†] Thomas Carell,*[,‡] and Wolfgang Zinth*[,†]

[†]BioMolecular Optics and Center for Integrated Protein Science, Ludwig-Maximilians- Universität München Oettingenstrasse 67, 80538 München, Germany

[‡]Center for Integrated Protein Science at the Department of Chemistry, Ludwig-Maximilians-Universität München, Butenandtstrasse 5-13, 81377 München, Germany

Supporting Information

ABSTRACT: UV-induced Dewar lesion formation is investigated in single- and double-stranded oligonucleotides with ultrafast vibrational spectroscopy. The quantum yield for the conversion of the (6−4) lesion to the Dewar isomer in DNA strands is reduced by a factor of 4 in comparison to model dinucleotides. Time resolved spectroscopy reveals a fast process in the excited state with spectral characteristics of bases which are adjacent to the excited (6−4) lesion. These kinetic components have large amplitudes and indicate that an additional quenching channel acts in the stranded DNA systems and reduces the Dewar formation yield. Presumably relaxation evolves via a charge transfer to the neighboring guanine and the paired cytosine participates in a double-stranded oligomer. Changes in the decay of the relaxed excited electronic state of the (6−4) chromophore point to modifications in the excited state energy landscape which may lead to an additional reduction of the Dewar formation yield.

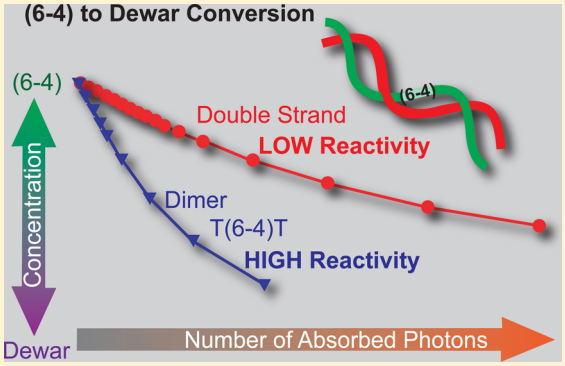

1. INTRODUCTION

UV-light absorption in DNA strands is known to induce a variety of photochemical reactions, leading to a multitude of photolesions which may induce cancer or cell death.[1−3] The most frequent photolesions are cyclobutane pyrimidine dimers (CPD) and (6−4) lesions between two neighboring pyrimidine bases.[2−5] A secondary photolesion is the Dewar valence isomer generated by photoconversion of the (6−4) lesion (Scheme 1a). The basis for Dewar lesion formation is a characteristic absorption band of the (6−4) lesion around 325 nm for the TT and 315 for the TC lesion. This unique absorption band is in the UV-A spectral region, where the solar irradiation on the earth surface is much higher than in the UV−B and UV−C region. Excitation of the (6−4) lesion at this wavelength leads to the effective conversion of the (6−4) chromophore to the Dewar valence isomer with a high quantum yield of 5−8% (measured in dinucleotides, Scheme 1a).[6] In addition to this, it is currently believed that the (6−4) lesion acts also as a triplet (photo)sensitizer upon photoexcitation to give the CPD lesion.[7] Understanding the excited state decay pathways and kinetics of the (6−4) lesion is therefore of high biological importance.[8,9]

In a series of recent studies with synthetic thymine dinucleotide Tc(6−4)T lesions containing a bioisosteric (6−4) lesion analogue (Scheme 1b) by ultrafast spectroscopy and quantum-chemistry[6,10,11] it was shown that the Tc(6−4)T excited state decays on the hundred picosecond time scale, forming the Dewar valence isomer and triplet states in an activated process. Quantum chemical calculations showed finally that the strain imposed on the (6−4)-chromophore by the backbone is of major importance for Dewar formation. This result is in line with the experimental observation that no Dewar product was observed after cleaving the backbone linkage within the (6−4) lesion.[6,10] A more recent publication reports the quantitative conversion of also unconstrained thymine photoproducts to the Dewar valence isomer.[12] While all these studies were so far performed with (6−4)-dinucleotides, we provide here data about the Dewar formation process in larger DNA single and double strand systems. This allows us to obtain deeper information on how the embedding of the (6−4) lesion in DNA influences the Dewar formation process.

We show that the lifetime of the excited electronic state is again in the subnanosecond to nanosecond range. However, the quantum yield of the Dewar formation is drastically reduced when going from model dinucleotides to DNA single and double strands. Femtosecond-infrared spectroscopy shows that the excited state of the (6−4)-chromophore is partially quenched by charge transfer to the neighboring bases. Together with changes in the geometry of the reactive excited state of the (6−4)-chromophore this may cause the reduction of the Dewar formation yield.

Received: May 17, 2015
Revised: June 20, 2015
Published: June 23, 2015

DOI: 10.1021/acs.jpcb.5b04694
J. Phys. Chem. B 2015, 119, 8685−8692

Scheme 1. (a) Photochemical Reaction of the Dinucleotide Tp(6-4)T Leading to the Dewar Isomer Tp(Dewar)T, (b) (6-4) Lesion Dinucleotide with the Formacetal Backbone Tc(6-4)T, and (c) Sequences of Single Strand (6-4)ss and Double Strand (6-4)ds Containing a (6-4) Lesion

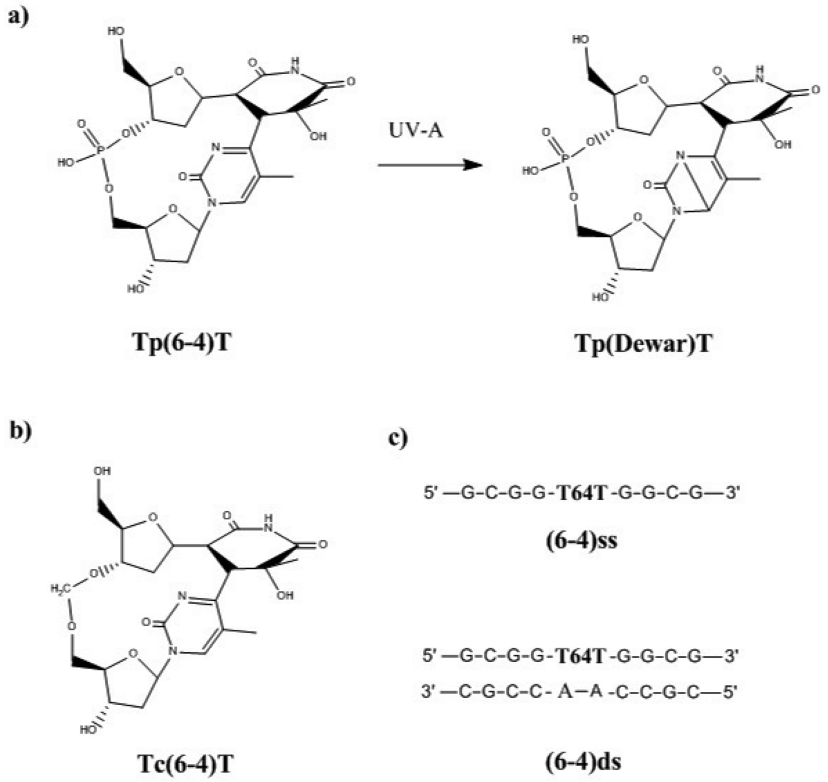

2. EXPERIMENTAL SECTION

Sample Preparation and Characterization. (6−4) lesion formation: GCGGTTGGCG, CGCCAACCGC and TT oligonucleotides used as the starting compounds were purchased from Metabion GmbH. UV-irradiation of these compounds was used to prepare the (6−4)-containing strands and Tp(6−4)T. The irradiation experiments were performed in the glovebox under anaerobic conditions.[13] The oligonucleotides were dissolved in degassed water (25 μM for GCGGTTGGCG and 125 μM for TT) and irradiated with a UV lamp (Vilber Luormat VL-215C, 2 × 15 W, 254 nm tubes) at a distance of 10 cm in Petri dishes, which were cooled by cooling packs. An irradiation time of 18 h for the GCGGTTGGCG oligonucleotides yielded maximum conversion to the (6−4) lesion. The TT dinucleotide illumination time was adjusted to 4 h. The irradiated solutions were lyophilized and purified by preparative reverse phase HPLC under the described conditions. For double strand formation the GCGGT64TGGCG was annealed with CGCCAACCGC over 3 h (85 → 20 °C) prior to the spectroscopic measurement.

HPLC Conditions. All analytical and preparative HPLC runs were performed on Water HPLC system using Nucleodur columns (250 × 4 mm, C18ec, particle size 3 μm, or 250 × 10 mm, C18ec, 5 μm) from Machery Nagel. Eluting buffer for the HPLC were buffer A (0.1 M triethylammonium acetate (TEAA) in H2O) and buffer B (0.1 M TEAA in H2O/MeCN 20/80). A flow of 0.5 mL/min and 5 mL/min was used for the analytical and preparative HPLC, respectively. For the purification of the (6−4) lesion a gradient of 0−17% B in 38 min was used. The elution was monitored at 260 and 325 nm, which is characteristic for the (6−4) lesion.

Melting Curves. DNA-melting temperature was determined by using a Carey 100 Biospectrophotometer equipped with Carey temperature controller, sample transport accessory and multi cell block (Varian). The melting experiments on the two complementary DNA oligomers (GCGGT64TGGCG and CGCCAACCGC) have shown that the system acquires a double-stranded conformation at room temperature even if the central (6−4) lesion would locally disturb the pairing of the two strands.

Stationary Spectroscopy. The infrared spectra were recorded on a Fourier transform infrared (FTIR) spectrometer (Model IFS 66, Bruker) in 100 μm CaF_2 cuvettes. All the samples were dissolved in 50 mM phosphate buffer. IR-experiments were performed in D_2O buffer. UV/vis spectra were recorded on a PerkinElmer Lambda 750 spectrophotometer.

Quantum Yield Determination. The quantum yield of the Dewar formation in all samples was determined via UV/vis spectroscopy. Since the Dewar valence isomer was found to be the only photoproduct, the yield for Dewar formation equals the destruction yield of the (6−4)-chromophore determined by measuring the absorbance decrease of the (6−4) marker band at 325 nm. The result was confirmed in a control experiment where the rise of the Dewar marker band in the IR at 1787 cm^{-1} was monitored upon extended illumination (SI4). In the experiment the (6−4)-sample was dissolved in H_2O phosphate buffer to an optical density of 0.4−0.5 OD at 325 nm in a 1 cm quartz cuvette. The solution was irradiated with light at 325 nm from a OPO system (NT242, Ekspla) (1 mW average power).

DOI: 10.1021/acs.jpcb.5b04694
J. Phys. Chem. B 2015, 119, 8685−8692

The absorbed light power was determined by recording the difference of the laser power before and after the cuvette, and suitable correction for reflection of the cuvette windows and buffer absorption. The absorbance change at 325 nm of the (6–4) lesion was determined after defined irradiation times by recording the UV/vis spectra. The corresponding concentrations were calculated using an extinction coefficient of 4000 1/Mcm. The concentration is plotted against the absorbed photons. From the initial slope of this graph the relative quantum yield is calculated. This method was verified by applying it to an actinometer compound of known quantum yield (1,3-Dimethyluracil photohydration in aqueous solution[14]).

Ultrafast Spectroscopy. The time-resolved infrared experiments are based on a Ti-sapphire laser-amplifier system (Spitfire Pro, Spectra Physics, central wavelength ~800 nm, 100 fs, 1 kHz). The excitation pulse at 325 nm was generated by a two stage noncollinear optical parametric amplifier (NOPA) followed by frequency doubling. To probe the absorption of the sample, a tunable mid infrared (3–11 μm) pulse is used, which is generated by optical parametric amplification and difference frequency mixing. The excitation pulses passed a 10 cm thick rod of fused silica to increase the pulse duration. This reduces the effect of multiphoton and multistep excitation and avoids artifacts due to nonlinear processes, but reduces the temporal resolution to ca. 1 ps. The excitation pulses were focused (diameter 150 μm) and overlaid with the probe pulse (diameter 90 μm) at the sample position. All measurements are performed under magic angle conditions. The transmitted probe pulses were spectrally dispersed with an imaging spectrograph (Bruker, Chromex 250 IS) and detected with a 64-channel MCT array (Infrared Systems Development, IR-0144). For the measurement a BaF_2 flow cuvette with an optical path length of 100 μm was used, where the sample was exchanged between consecutive excitation pulses. All experiments were performed at room temperature.

Data Analysis. The time-resolved absorbance changes were collected as an array of absorption changes for different probing frequencies ν and delay times t_D. The data at $t_D > 5$ ps were globally fitted with two exponentials and a constant offset representing long-lasting absorption changes from irreversible processes or triplet states:

$$\Delta A(\nu, t_D) = \sum_{i=1}^{2} D_i(\nu) \exp\left(-\frac{t_D}{\tau_i}\right) + D_3(\nu)$$

For each time constant, an amplitude spectrum $D_i(\nu)$ is determined in the fit, which represents the difference spectrum of the process (decay associated difference spectrum, DADS) used in this publication.

3. RESULTS

The investigated dinucleotides and short oligonucleotides (Scheme 1c) with the (6–4) lesion in a central position were prepared as described in the Experimental Section. The sequence GCGGTTGGCG was used as starting material because it gives significant yields of the T(64)T lesion upon direct UV-irradiation. The purified single strand GCGGT64TGGCG, (abbreviated as (6–4)ss) containing the (6–4) lesion in the central TT position, was annealed with its opposite strand CGCCAACCGC forming stable duplexes ((6–4)ds) at room temperature (see Supporting Information, part SI1).

The quantum yields of the isomerization of the dimer Tp(6–4)T, the (6–4)ss and (6–4)ds were determined as described above and compared to the Tc(6–4)T analogue described in former publications[6] (for yields see Table 1, for details see the Experimental Section). In Figure 1 the change in (6–4) concentration is plotted versus the number of absorbed photons. It is evident that the concentration of the (6–4) chromophore in the dimers decreases very rapidly. A much slower decrease is observed for the (6–4) lesions in single- and double-stranded DNA. From the initial slope of the concentration reduction we deduced the relative quantum yields for the (6–4) chromophore conversion. The two dinucleotides show similar quantum yields of $\eta_{Dewar,\,rel}$ = 1.0 and 0.8. For the single- and double-stranded DNA, a pronounced reduction of the yield by a factor of more than four relative to the dinucleotides is found ($\eta_{Dewar,\,rel}$ = 0.2). Interestingly, the quantum yield of the Dewar formation is very similar in single and double strands.

Table 1 shows that the Dewar formation yield strongly changes when the (6–4) lesion is embedded in DNA. While the difference in the backbone structure of the dinucleotides (formacetal in the Tc(6–4)T versus phosphate in Tp(6–4)T) cause only small changes of the quantum yields, a ca. 4-fold reduction of the yield is found in stranded and double-stranded DNA. This difference may be due to the geometrical change imposed by the structural confinements in longer DNA strands or due to the presence of neighboring bases in the DNA strand.

Table 1. Relative Reaction Quantum Yields $\eta_{Dewar,rel}$ Deduced from the Decay of the (6-4) UV-Absorption at 325 nm upon Extended Illumination in Different Systems Used as an Indication for Dewar Formation[a]

structure	relative quantum yield
Tc(6–4)T	1
Tp(6–4)T	0.8
(6–4)ss	0.2
(6–4)ds	0.2

[a]The relative quantum yield $\eta_{Dewar,rel}$ = 1 corresponds to an absolute yield of η_{Dewar} = 5 to 8%.

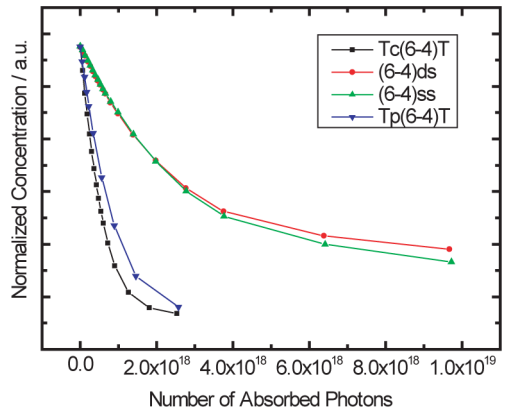

Figure 1. Concentration of the (6–4)-chromophore of the different samples upon irradiation at 325 nm plotted versus the number of absorbed photons. The initial slope is directly related to the quantum efficiency for the photochemical conversion of the (6–4)-chromophore.

DOI: 10.1021/acs.jpcb.5b04694
J. Phys. Chem. B 2015, 119, 8685–8692

We performed time-resolved experiments to decipher the reaction dynamics. They were initiated by selective excitation of the (6–4) lesion via its absorption band at 325 nm (SI2). The subsequent absorption changes are monitored by infrared spectroscopy which gives information about electronic[15−17] and structural changes.[18,19] Figure 2a shows the transient

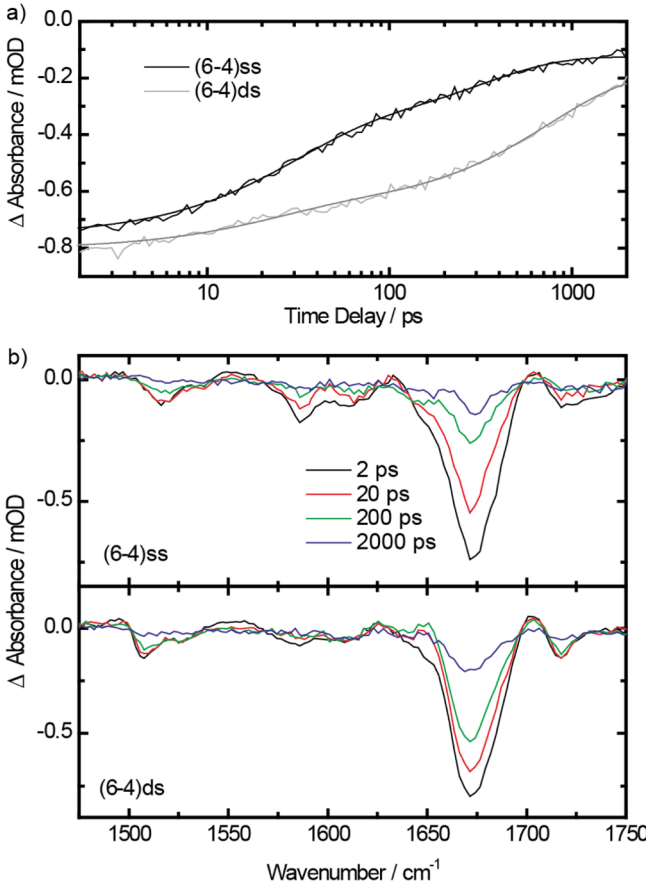

Figure 2. (a) Ground state bleach recovery at 1671 cm^{-1} for the (6–4) lesion in single- and double-stranded DNA. Solid lines: biexponential fit of the experimental data using the time constants given in the text. (b) Transient spectra recorded at the indicated delay times for (6–4) lesion in single- and double-stranded DNA.

absorption changes recorded at 1671 cm^{-1}, i. e. at a position with a strong absorption of the (6–4) lesion (see Figure 2b). This absorption bleaches due to the excitation. In the single-stranded system (6–4)ss, (Figure 2a, black curve) the decay of the bleach is faster than in the double strand (6–4)ds (Figure 2a, gray curve). More detailed information was obtained from absorption difference spectra, recorded at different delay times over a broad spectral range and from the modeling of the data (Figure 2b). We performed a global modeling of the transient absorption changes using two exponential functions and an offset due to product and triplet formation. The corresponding fit amplitudes and the decay associated difference spectra (DADS) are plotted in Figure 3 for (6–4)ss and (6–4)ds. The modeling yields time constants of τ_1 = 20 ps and τ_2 = 260 ps for (6–4)ss and a long-living component (SI5). τ_1 = 16 ps and τ_2 = 750 ps are found for the double strand (6–4)ds. In a separate experiment we tried to monitor the appearance of the Dewar photoproduct via its marker band at $1/\lambda$ = 1787 cm^{-1}. We could not resolve unambiguously the rise of this marker band, apparently due to the very small efficiency for Dewar formation in the stranded systems (see above) and the small extinction coefficient of the 1787 cm^{-1} band. However, there were indications for the Dewar band visible in the offset spectrum (Supporting Information, part SI5).

Although the Dewar formation is not directly recorded via its marker band, the decay of the excited state of the (6–4) lesion is well visible. Furthermore, the infrared spectra provide additional information about intermediate states because they can distinguish between different DNA bases due to the narrow absorbance bands.

In the DADS, negative bands are caused by the bleach of ground state absorption. Positive bands are created by excited states, intermediates or photoproducts. The excitation decays of the (6–4) lesion in single- and double-stranded DNA show processes on two different time scales with very different spectral features. The DADS of the slow decay (Figure 3, parts c and f, time constants τ_2 = 260 and 750 ps for (6–4)ss and (6–4)ds, respectively) exhibit features which are similar to those observed recently for Tc(6–4)T (see dashed curves;[6] for an interpretation of the various bands, see refs 10 and 11). Upon decay of the excited (6–4)-state followed by Dewar formation in the dinucleotide we see the recovery bands of the original (6–4)-absorption bands at 1666, 1612, 1592, and 1516 cm^{-1}. Within DNA oligomers (6–4)ss and (6–4)ds a strong bleach appears around 1670 cm^{-1}. Other bleaching bands are also visible in the DNA strands but they are much weaker. Therefore, we assigned the slow decay process of the DNA samples to the final decay of the excited (6–4) lesion. In the offset spectrum, describing the final state reached on the few nanosecond time scale, we also find a negative signal at the position 1670 cm^{-1} of the (6–4)-absorption bands pointing to incomplete recovery of the (6–4) state. Apparently, this bleach is due to the formation of the Dewar valence isomer or other long-lived product states such as triplet states.

Of special interest is the fast decaying component with a time constant in the τ_1 = 20 ps range where the DADS are shown for (6–4)ss and (6–4)ds in Figure 3, parts b and e, respectively. Such a kinetic component was not observed in the experiment with the dinucleotides Tc(6–4)T. These DADS show pronounced bleaches at additional spectral positions, indicative for specific nucleobases in the strands (SI3).[20−22] For (6–4)ss we observe the bleach of bands at 1673 and 1583 cm^{-1}. These positions are related to the base guanine G (see Figure 3a), adjacent to the (6–4) lesion in the single strand. The double strand (6–4)ds bleach is observed at 1680, 1650, 1581, and 1503 cm^{-1}. Again two of these positions (at 1680 and 1581 cm^{-1}) can be related to the absorption bands of G-base in the duplex. The pronounced band at 1650 cm^{-1} (of similar amplitude as the band from G at 1680 cm^{-1}) and the weak band at 1503 cm^{-1} can be assigned to cytosine (C). Surprisingly, a similar bleach of a C-band was not observe in the experiment with a single strand. As a consequence we may assign this bleach to the C in the counter strand, paired to the G adjacent to the (6–4) lesion. This observation indicates that not only the neighboring G-base but also the C-based connected by Watson–Crick base-pairing is involved in the decay of the excited (6–4) lesion. The DADS of Figure 3, parts b and e, also show contributions from a bleach of the (6–4)-state, indicating that the corresponding short-living state involves the simultaneous excitation of the bases (G and/or C) and the (6–4)-chromophore.

DOI: 10.1021/acs.jpcb.5b04694
J. Phys. Chem. B 2015, 119, 8685–8692

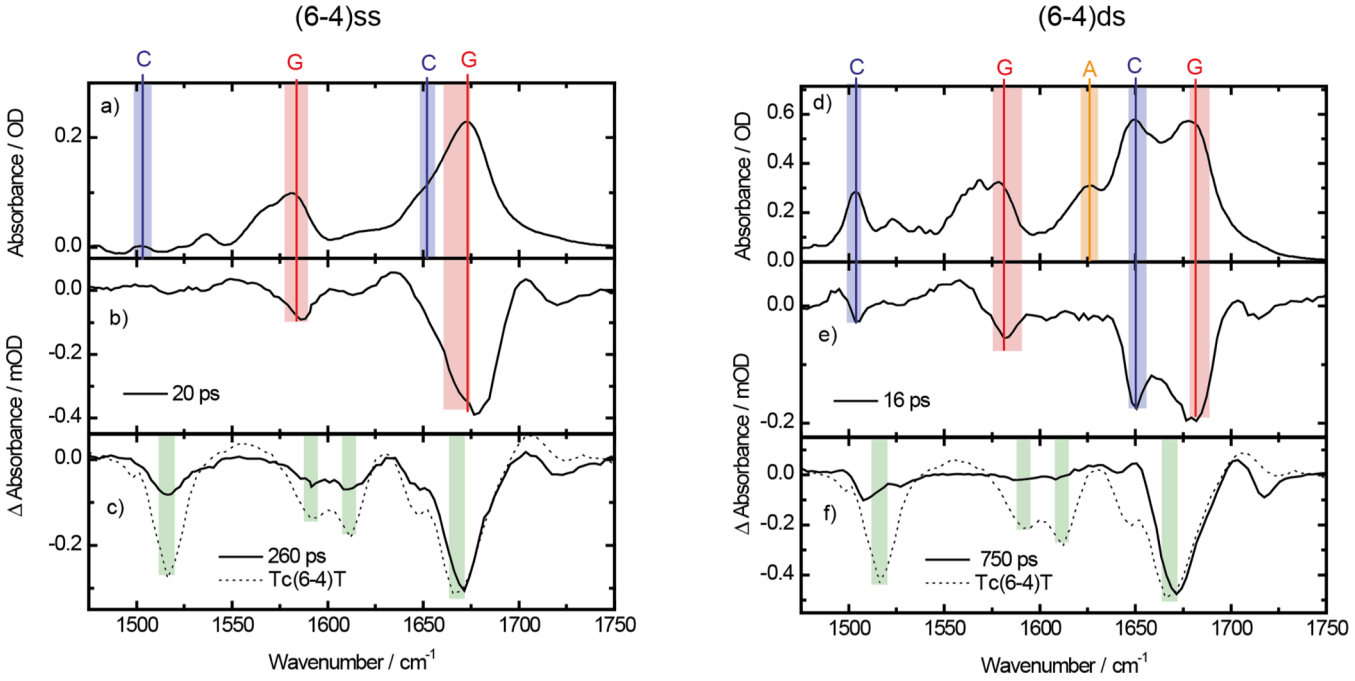

Figure 3. Absorption spectra in the IR of the strands (6−4)ss (a) and (6−4)ds (d). Colored bars show the spectral position of the nucleobases adenine, guanine and cytosine in corresponding strands according to the literature (SI3). Decay associated difference spectra (DADS) of the single strand sample (6−4)ss (b and c) and the double strand sample (6−4)ds (e and f), respectively. The dashed curves in parts c and f show the DADS of the 130 ps kinetic component of the sample Tc(6−4)T investigated in Haiser et al.[6] The green bars indicate bands of the (6−4) lesion also visible in the long-time DADS of the (6−4)ss and (6−4)ds sample.

4. DISCUSSION

For the interpretation of the experimental observations on the 100 ps time scale we refer to the reaction model of the (6−4)-decay and Dewar formation presented in Haiser et al.[6] and Fingerhut et al.[10,11] The model is depicted schematically in Scheme 2 on the right part. For the dimer Tc(6−4)T, the initial excitation of the Franck−Condon region (state $(6-4)^*_{FC}$) is followed by a rapid relaxation on the excited state potential energy surface toward the minimum (state $(6-4)^*_{rel}$), where the system resides for about 130 ps. Further reactions to the Dewar product and/or the back-reaction to the ground-state occurs via conical intersections ($CoIn_{Dewar}$), accessible after overcoming respective barriers. The excited state energy landscape and consequently the reaction yield for Dewar formation strongly depend on geometrical constrains and the acting forces. Therefore, it is not surprising that the incorporation of the (6−4)-chromophore into a DNA strand leads to a reduction of the reaction yield. Apparently the accessibility of the different CoIn is changed by increasing the barrier heights. Additionally there might be a change of the bifurcation between Dewar formation and back-reaction to the ground-state at $CoIn_{Dewar}$.

Scheme 2. Level Scheme for the Processes Occurring after Excitation of the (6−4) Lesion[a]

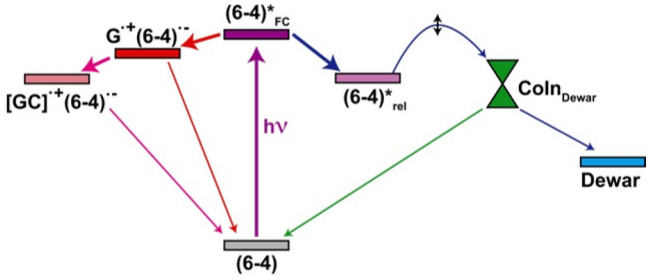

[a]For a dimer, quantum chemical calculations have shown that the reaction proceeds over the states ($(6-4)^*_{FC}$ and $(6-4)^*_{rel}$) and the conical intersection $CoIn_{Dewar}$ shown on the right part of the scheme and exhibit a relatively high probability of Dewar formation. When the (6−4) lesion is incorporated into DNA-strands, further intermediates (see left part) become accessible which lead to additional quenching of the initially excited (6−4)*FC state. Other changes in the excited state surface in the range between (6−4)*rel and the CoIn (e.g., increase of barrier heights, change of the character of the CoIn) induced by the geometric constrains of the strands may lead to a further decrease of the Dewar formation yield.

While the changes in dynamics related to the decay of the excited (6−4)* states from 130 ps in Tc(6−4)T to 260 ps in (6−4)ss or 750 ps in (6−4)ds may be explained by modifications of the excited state potential energy scheme, the appearance of the intense absorption dynamics on the time scale of 20 ps and the surprising contribution of G- and/or C-base in close vicinity to the (6−4) lesion are interesting.

There are different possibilities to describe the simultaneous absorption transients related to the excited (6−4)-chromophore and to the base G upon excitation at 325 nm. A direct excitation of base G cannot explain the observations since the absorption of G at this wavelength is extremely weak. An indirect population of the $\pi\pi^*$ state of G by excitation transfer (FRET) from (6−4)* can also be excluded due to the energetic mismatch and the missing spectral overlap. However, the population of a charge transfer (CT) state involving the guanine cation $G^{\bullet+}$ and the $(6-4)^{\bullet-}$ anion appears possible, considering the low oxidation potential of G. Indeed, photoinduced charge transfer between chromophores in DNA and nucleobases have been known for a long time.[23−25] In addition, photoinduced charge transfer between neighboring

DOI: 10.1021/acs.jpcb.5b04694
J. Phys. Chem. B 2015, 119, 8685−8692

bases were recently reported as major decay channels for excited $\pi\pi^*$ state in DNA single strands.[26−29] Thus, the charge pair $G^{\bullet+}(6-4)^{\bullet-}$ is the most likely excited state involving G and the (6−4)-chromophore simultaneously. Here the $G^{\bullet+}$ cation becomes visible by the bleach of the G absorption band at 1683 cm^{-1}. Unfortunately the marker band[26,30,31] of the $G^{\bullet+}$ cation at 1704 cm^{-1} cannot be used to identify $G^{\bullet+}(6-4)^{\bullet-}$, since this band overlaps with the (6−4)*-absorption features. The rapid recovery of the absorption bleach assigned to $G^{\bullet+}(6-4)^{\bullet-}$ on the 20 ps time scale can be explained by charge back-transfer. In corresponding single strand-systems with transient population of charge transfer states similar time constants were found.[26−29] The fast charge separation and the much slower charge recombination are well explained by semiclassical nonadiabatic electron transfer theory.[32]

The population of the CT-state $G^{\bullet+}(6-4)^{\bullet-}$ has to occur from the initially populated and rapidly decaying excited state $(6-4)^*_{FC}$. Otherwise the bleach of G should extend to the hundred picosecond time scale of the decay of $(6-4)^*_{rel}$. Apparently the drop in energy upon relaxation from $(6-4)^*_{FC}$ to $(6-4)^*_{rel}$ prevents population of the CT-state from the long-lived $(6-4)^*_{rel}$. The large amplitude of the 20 ps DADS indicates that a considerable fraction (about 50%) of the initially excited molecules reacts to the CT-state, which is quickly deactivated to the ground-state by charge back-transfer. Therefore, this fraction cannot contribute to Dewar formation. Thus, the CT-channel supplies an additional deactivation pathway that reduces Dewar formation reaction in stranded DNA. This is a major reason for the observed reduction of the quantum yield to the Dewar lesion (see Table 1).

The most striking observation with the double-stranded system is the combined bleach of the absorption of the C, G-bases and the (6−4)-chromophore. The bleach of the two complementary bases G and C in (6−4)ds indicates that the excitation is spread over the Watson−Crick-paired bases and the (6−4)-chromophore. If we assume that the optical excitation of the (6−4)-chromophore to the Franck−Condon state $(6-4)^*_{FC}$ is followed initially by charge separation to give $G^{\bullet+}(6-4)^{\bullet-}$, the bleach of the absorption band of cytosine suggests that a secondary reaction occurs that involves cytosine. The ground state bleach of cytosine builds up within the temporal resolution of 1 ps, indicating that the hydrogen bond pattern between the Watson−Crick G:C base pair is modified, while keeping the positive charge. We therefore denote this state formally as $[GC]^{\bullet+}(6-4)^{\bullet-}$ in agreement with reaction data that show such interstrand proton transfers.[21,22] Three models were discussed in the literature that could explain this observation. In two models the proton transfer originates directly from the photoexcited $\pi\pi^*$ state of one base.[33−35] These models may not be valid in the present situation since the original excitation in our experiment occurs at the (6−4)-chromophore and an excitation transfer to the neighboring G can be excluded (see above). The third model[36,37] involves an initial intrastrand charge transfer followed by an interstrand proton transfer. The only difference to the present situation is the negative charge located at the (6−4)-chromophore. A prerequisite for the model is, however, an intact double helical structure in the vicinity of (6−4) chromophore. Although the (6−4) lesion distorts the DNA structure, the B-form of the helix is indeed preserved at the 3′ end, as shown by NMR spectroscopy.[38] Therefore, we assume an intact G-C base pairing at the 3′ end of the (6−4) lesion. The reason for the proton transfer is that $G^{\bullet+}$ is more acidic[39,40] than G favoring the state $[GC]^{\bullet+}(6-4)^{\bullet-}$. Thus, a proton coupled electron transfer (PCET) explains a bleach of the complete base pair. Indeed such a proton-coupled electron transfer has been discovered recently in double-stranded DNA where the $G^{\bullet+}$ was produced from a Ruthenium-complex attached to the DNA.[41]

The decay of the $[GC]^{\bullet+}(6-4)^{\bullet-}$ state with a time constant of 16 ps must involve the back-transfer of the electron and the rearrangement of the hydrogen bond pattern. The corresponding time constant is of the order of magnitude observed previously in double-stranded systems for such processes. Remaining differences in recombination times are well explained within semiclassical nonadiabatic electron transfer theory by the changed energetics.

In conclusion, Dewar formation in single and double strands containing the (6−4) lesion is strongly reduced as compared to dinucleotides. In the DNA strands geometries and interactions are modified. In particular, the close distance between adjacent and stacked bases reduces the Dewar formation yield dramatically. The corresponding changes in the energy landscape of the excited state of the (6−4) lesion and the formation of additional quenching channels via charge transfer states help to protect the integrity of our genetic code.

■ ASSOCIATED CONTENT

Supporting Information

Additional supporting figures and tables, showing a melting curve, UV−vis and IR spectra, and decay-associated difference spectra. The Supporting Information is available free of charge on the ACS Publications website at DOI: 10.1021/acs.jpcb.5b04694.

■ AUTHOR INFORMATION

Corresponding Authors

*(W.Z.) E-mail: wolfgang.zinth@physik.uni-muenchen.de.
*(T.C.) E-mail: thomas.carell@cup.uni-muenchen.de.

Author Contributions

The manuscript was written through contributions of all authors. All authors have given approval to the final version of the manuscript.

Funding

This work was supported by the Deutsche Forschungsgemeinschaft through the Sonderforschungsbereich “Dynamics and Intermediates of Molecular Transformations” SFB 749, A4 and A5, the Clusters of Excellence “Center for Integrated Protein Science Munich”, and the “Munich-Centre for Advanced Photonics”.

Notes

The authors declare no competing financial interest.

■ REFERENCES

(1) Taylor, J. S. Unraveling the Molecular Pathway from Sunlight to Skin Cancer. *Acc. Chem. Res.* **1994**, *27* (3), 76−82.
(2) Pfeifer, G. P.; You, Y.-H.; Besaratinia, A. Mutations Induced by Ultraviolet Light. *Mutat. Res. Mol. Mech. Mutagen.* **2005**, *571* (1−2), 19−31.
(3) Schreier, W. J.; Gilch, P.; Zinth, W. Early Events of DNA Photodamage. *Annu. Rev. Phys. Chem.* **2015**, *66* (1), 497−519.
(4) Ravanat, J.-L.; Douki, T.; Cadet, J. Direct and Indirect Effects of UV Radiation on DNA and Its Components. *J. Photochem. Photobiol., B* **2001**, *63* (1−3), 88−102.

DOI: 10.1021/acs.jpcb.5b04694
J. Phys. Chem. B 2015, 119, 8685−8692

(5) Kneuttinger, A. C.; Kashiwazaki, G.; Prill, S.; Heil, K.; Müller, M.; Carell, T. Formation and Direct Repair of UV-Induced Dimeric DNA Pyrimidine Lesions. *Photochem. Photobiol.* **2014**, *90* (1), 1−14.
(6) Haiser, K.; Fingerhut, B. P.; Heil, K.; Glas, A.; Herzog, T. T.; Pilles, B. M.; Schreier, W. J.; Zinth, W.; de Vivie-Riedle, R.; Carell, T. Mechanism of UV-Induced Formation of Dewar Lesions in DNA. *Angew. Chem., Int. Ed.* **2012**, *51*, 408−411.
(7) Vendrell-Criado, V.; Rodríguez-Muñiz, G. M.; Cuquerella, M. C.; Lhiaubet-Vallet, V.; Miranda, M. A. Photosensitization of DNA by 5-Methyl-2-Pyrimidone Deoxyribonucleoside: (6−4) Photoproduct as a Possible Trojan Horse. *Angew. Chem., Int. Ed.* **2013**, *52*, 6476.
(8) Meador, J. A.; Baldwin, A. J.; Pakulski, J. D.; Jeffrey, W. H.; Mitchell, D. L.; Douki, T. The Significance of the Dewar Valence Photoisomer as a UV Radiation-Induced DNA Photoproduct in Marine Microbial Communities. *Environ. Microbiol.* **2014**, *16* (6), 1808−1820.
(9) Qin, X.; Zhang, S.; Zarkovic, M.; Nakatsuru, Y.; Shimizu, S.; Yamazaki, Y.; Oda, H.; Nikaido, O.; Ishikawa, T. Detection of Ultraviolet Photoproducts in Mouse Skin Exposed to Natural Sunlight. *Jpn. J. Cancer Res.* **1996**, *87* (7), 685−690.
(10) Fingerhut, B. P.; Herzog, T. T.; Ryseck, G.; Haiser, K.; Graupner, F. F.; Heil, K.; Gilch, P.; Schreier, W. J.; Carell, T.; de Vivie-Riedle, R.; et al. Dynamics of Ultraviolet-Induced DNA Lesions: Dewar Formation Guided by Pre-Tension Induced by the Backbone. *New J. Phys.* **2012**, *14* (6), 065006.
(11) Fingerhut, B. P.; Oesterling, S.; Haiser, K.; Heil, K.; Glas, A.; Schreier, W. J.; Zinth, W.; Carell, T.; Vivie-Riedle, R. de. ONIOM Approach for Non-Adiabatic on-the-Fly Molecular Dynamics Demonstrated for the Backbone Controlled Dewar Valence Isomerization. *J. Chem. Phys.* **2012**, *136* (20), 204307.
(12) Douki, T.; Rebelo-Moreira, S.; Hamon, N.; Bayle, P.-A. DNA Photochemistry: Geometrically Unconstrained Pyrimidine (6−4) Pyrimidone Photoproducts Do Photoisomerize. *Org. Lett.* **2015**, *17* (2), 246−249.
(13) Glas, A. F.; Schneider, S.; Maul, M. J.; Hennecke, U.; Carell, T. Crystal Structure of the T(6−4)C Lesion in Complex with a (6−4) DNA Photolyase and Repair of UV-Induced (6−4) and Dewar Photolesions. *Chem.—Eur. J.* **2009**, *15* (40), 10387−10396.
(14) Kuhn, H. J.; Braslavsky, S. E.; Schmid, R. Chemical Actinometry (IUPAC Technical Report). *Pure Appl. Chem.* **1989**, *61*, 187−210.
(15) Bucher, D. B.; Pilles, B. M.; Pfaffeneder, T.; Carell, T.; Zinth, W. Fingerprinting DNA Oxidation Processes: IR Characterization of the 5-Methyl-2′-Deoxycytidine Radical Cation. *ChemPhysChem* **2014**, *15* (3), 420−423.
(16) Pilles, B. M.; Bucher, D. B.; Liu, L.; Clivio, P.; Gilch, P.; Zinth, W.; Schreier, W. J. Mechanism of the Decay of Thymine Triplets in DNA Single Strands. *J. Phys. Chem. Lett.* **2014**, *5* (9), 1616−1622.
(17) Deeg, A. A.; Rampp, M. S.; Popp, A.; Pilles, B. M.; Schrader, T. E.; Moroder, L.; Hauser, K.; Zinth, W. Isomerization- and Temperature-Jump-Induced Dynamics of a Photoswitchable B-Hairpin. *Chem.—Eur. J.* **2014**, *20* (3), 694−703.
(18) Schreier, W. J.; Schrader, T. E.; Koller, F. O.; Gilch, P.; Crespo-Hernandez, C. E.; Swaminathan, V. N.; Carell, T.; Zinth, W.; Kohler, B. Thymine Dimerization in DNA Is an Ultrafast Photoreaction. *Science* **2007**, *315* (5812), 625−629.
(19) Schreier, W. J.; Kubon, J.; Regner, N.; Haiser, K.; Schrader, T. E.; Zinth, W.; Clivio, P.; Gilch, P. Thymine Dimerization in DNA Model Systems: Cyclobutane Photolesion Is Predominantly Formed via the Singlet Channel. *J. Am. Chem. Soc.* **2009**, *131* (14), 5038−5039.
(20) Banyay, M.; Sarkar, M.; Gräslund, A. A Library of IR Bands of Nucleic Acids in Solution. *Biophys. Chem.* **2003**, *104* (2), 477−488.
(21) Bucher, D. B.; Schlueter, A.; Carell, T.; Zinth, W. Watson−Crick Base Pairing Controls Excited-State Decay in Natural DNA. *Angew. Chem., Int. Ed.* **2014**, *53* (42), 11366−11369.
(22) Bucher, D. B.; Schlueter, A.; Carell, T.; Zinth, W. In natürlicher DNA wird der Zerfall des angeregten Zustands durch Watson-Crick-Basenpaarung bestimmt. *Angew. Chem.* **2014**, *126* (42), 11549−11552.
(23) Wan, C.; Fiebig, T.; Kelley, S. O.; Treadway, C. R.; Barton, J. K.; Zewail, A. H. Femtosecond Dynamics of DNA-Mediated Electron Transfer. *Proc. Natl. Acad. Sci. U.S.A.* **1999**, *96* (11), 6014−6019.
(24) Wan, C.; Fiebig, T.; Schiemann, O.; Barton, J. K.; Zewail, A. H. Femtosecond Direct Observation of Charge Transfer between Bases in DNA. *Proc. Natl. Acad. Sci. U.S.A.* **2000**, *97* (26), 14052−14055.
(25) Lewis, F. D.; Liu, X.; Liu, J.; Miller, S. E.; Hayes, R. T.; Wasielewski, M. R. Direct Measurement of Hole Transport Dynamics in DNA. *Nature* **2000**, *406* (6791), 51−53.
(26) Bucher, D. B.; Pilles, B. M.; Carell, T.; Zinth, W. Charge Separation and Charge Delocalization Identified in Long-Living States of Photoexcited DNA. *Proc. Natl. Acad. Sci. U. S. A.* **2014**, 201323700.
(27) Doorley, G. W.; Wojdyla, M.; Watson, G. W.; Towrie, M.; Parker, A. W.; Kelly, J. M.; Quinn, S. J. Tracking DNA Excited States by Picosecond-Time-Resolved Infrared Spectroscopy: Signature Band for a Charge-Transfer Excited State in Stacked Adenine−Thymine Systems. *J. Phys. Chem. Lett.* **2013**, *4* (16), 2739−2744.
(28) Zhang, Y.; Dood, J.; Beckstead, A. A.; Li, X.-B.; Nguyen, K. V.; Burrows, C. J.; Improta, R.; Kohler, B. Efficient UV-Induced Charge Separation and Recombination in an 8-Oxoguanine-Containing Dinucleotide. *Proc. Natl. Acad. Sci. U.S.A.* **2014**, *111* (32), 11612−11617.
(29) Pilles, B. M.; Bucher, D. B.; Liu, L.; Gilch, P.; Zinth, W.; Schreier, W. J. Identification of Charge Separated States in Thymine Single Strands. *Chem. Commun.* **2014**, *50* (98), 15623−15626.
(30) Kuimova, M. K.; Cowan, A. J.; Matousek, P.; Parker, A. W.; Sun, X. Z.; Towrie, M.; George, M. W. Monitoring the Direct and Indirect Damage of DNA Bases and Polynucleotides by Using Time-Resolved Infrared Spectroscopy. *Proc. Natl. Acad. Sci. U.S.A.* **2006**, *103* (7), 2150−2153.
(31) Parker, A. W.; Lin, C. Y.; George, M. W.; Towrie, M.; Kuimova, M. K. Infrared Characterization of the Guanine Radical Cation: Finger Printing DNA Damage. *J. Phys. Chem. B* **2010**, *114* (10), 3660−3667.
(32) Zhang, Y.; Dood, J.; Beckstead, A. A.; Li, X.-B.; Nguyen, K. V.; Burrows, C. J.; Improta, R.; Kohler, B. Photoinduced Electron Transfer in DNA: Charge Shift Dynamics Between 8-Oxo-Guanine Anion and Adenine. *J. Phys. Chem. B* **2015**, *119*, 7491−7502.
(33) Douhal, A.; Kim, S. K.; Zewail, A. H. Femtosecond Molecular Dynamics of Tautomerization in Model Base Pairs. *Nature* **1995**, *378* (6554), 260−263, DOI: 10.1038/378260a0.
(34) Perun, S.; Sobolewski, A. L.; Domcke, W. Role of Electron-Driven Proton-Transfer Processes in the Excited-State Deactivation of the Adenine−Thymine Base Pair. *J. Phys. Chem. A* **2006**, *110* (29), 9031−9038.
(35) Sobolewski, A. L.; Domcke, W. Ab Initio Studies on the Photophysics of the Guanine−cytosine Base Pair. *Phys. Chem. Chem. Phys.* **2004**, *6* (10), 2763−2771.
(36) De La Harpe, K.; Crespo-Hernández, C. E.; Kohler, B. Deuterium Isotope Effect on Excited-State Dynamics in an Alternating GC Oligonucleotide. *J. Am. Chem. Soc.* **2009**, *131* (48), 17557−17559.
(37) Ko, C.; Hammes-Schiffer, S. Charge-Transfer Excited States and Proton Transfer in Model Guanine-Cytosine DNA Duplexes in Water. *J. Phys. Chem. Lett.* **2013**, *4* (15), 2540−2545.
(38) Lee, J.-H.; Bae, S.-H.; Choi, B.-S. The Dewar Photoproduct of Thymidylyl(3′→5′)- Thymidine (Dewar Product) Exhibits Mutagenic Behavior in Accordance with the "A Rule. *Proc. Natl. Acad. Sci. U.S.A.* **2000**, *97* (9), 4591−4596.
(39) Close, D. M. Calculated pKa's of the DNA Base Radical Ions. *J. Phys. Chem. A* **2013**, *117* (2), 473−480.
(40) Steenken, S. Electron-Transfer-Induced Acidity/basicity and Reactivity Changes of Purine and Pyrimidine Bases. Consequences of Redox Processes for DNA Base Pairs. *Free Radical Res. Commun.* **1992**, *16* (6), 349−379.
(41) Elias, B.; Creely, C.; Doorley, G. W.; Feeney, M. M.; Moucheron, C.; Kirsch-DeMesmaeker, A.; Dyer, J.; Grills, D. C.; George, M. W.; Matousek, P.; et al. Photooxidation of Guanine by a Ruthenium Dipyridophenazine Complex Intercalated in a Double-Stranded Polynucleotide Monitored Directly by Picosecond Visible

DOI: 10.1021/acs.jpcb.5b04694
J. Phys. Chem. B 2015, 119, 8685−8692

and Infrared Transient Absorption Spectroscopy. *Chem.—Eur. J.* **2008**, *14* (1), 369−375.

DOI: 10.1021/acs.jpcb.5b04694
J. Phys. Chem. B 2015, 119, 8685−8692